Ductile deformation of bedded anhydrite as revealed by strained nodule fabrics

W.M. SCHWERDTNER, J.T. VAN BERKEL AND J.G. TORRANCE

Thick bodies of bedded anhydrite mark three large thrusts and many other faults in the Eureka Sound fold-and-thrust belt, Canadian Arctic Islands. The anhydrite is an aggregate of irregular centimetre-scale nodules variously distorted by tectonic deformation. Near fault planes, the anhydrite is mylonitized, and its nodules are extremely flattened, sheared and folded. Here, finite-strain analysis proved impossible due to profound heterogeneity of deformation on the scale of a few centimetres. A similar problem is encountered in unfaulted evaporite diapirs where steep oblate nodules with axial ratios of >30 coalesce partly to form crude layers. At most localities within diapirs, the oblate and prolate nodules have axial ratios of <20 and can be used to delineate shape fabric patterns which are the net effect of compaction (virtual strain), evaporite diapirism and subsequent regional deformation.

W.M. Schwerdtner, Department of Geology, University of Toronto, Toronto, Ontario, Canada M53 1A1.
J.T. van Berkel, Vrije Universiteit Instituut voor Aardwetenschappen, 1007 MC Amsterdam, Nederland.
J.G. Torrance, Heath Steele Mines Ltd., P.O. Box 400, Newcastle, New Brunswick, Canada E1V 3M5.

Introduction

Evaporites are common in the thick sedimentary piles of Phanerozoic basins. Many lithified piles are folded, up-lifted and partly eroded, thereby exposing strained salt and anhydrite. These rocks form prominent outcrops in desert regions, and have been studied in northern Africa, Iran and the Canadian Arctic Islands (O'Brien 1957, Heim 1958, Talbot 1979, van Berkel et al. 1983, 1984). The authors are engaged in detailed field work in the eastern central Sverdrup Basin, Canadian High Arctic, to (1) study the mechanical role of bedded anhydrite in thrust zones, and (2) use strained anhydrite rocks as structural analogues of common meta-plutonites.

Anhydrite rocks are much more ductile under most tectonic conditions than clastic sedimentary rocks and carbonate rocks (Lotze 1957, p. 314–326, van Berkel et al. 1984). In association with salt and potash rocks, however, anhydrite proves to be relatively brittle and breaks after initial ductile flow (Lotze 1957, p. 314–326). The magnitude of total tectonic strain recorded by the nodule fabric reflects the degree to which anhydrite rocks served as a natural lubricant in the overall deformation of, and thrusting within, thick sedimentary piles (cf. Müller and Briegel 1980, Müller et al. 1981).

The subsiding Sverdrup Basin accumulated a sedimentary sequence of about 10 km thickness between the Lower Carboniferous and Upper Cretaceous, and its depocentre contains thick deposits of Carboniferous evaporites (Thorsteinsson 1974, Nassichuk and Davies 1980). Salt diapirs rose in the Mesozoic (Schwerdtner and Osadetz 1983, Jackson and Halls 1985), before the eastern half of the sedimentary pile was subjected to horizontal tectonism in the Lower Tertiary which created the Eureka Sound fold-and-thrust belt (Thorsteinsson and Tozer 1970).

Throughout the central Sverdrup Basin, nodular Carboniferous anhydrite is interbedded with limestone and exposed in diapirs and/or fault zones (Fig. 1–2). Here the nodules have various shapes and orientations, which are mainly related to the state of total strain (van Berkel et al., 1986). The coalescence of nodules with extreme axial ratios of >30 gives rise to laminated rocks which resemble banded gneiss. This suggests that nodular anhydrite is a structural analogue of coarse-grained meta-plutonic
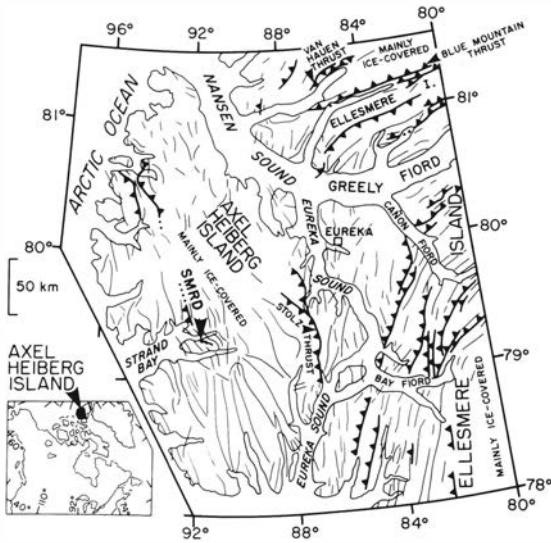
Figure 1. Eureka Sound fold-and-thrust belt (after van Berkel 1986, fig. 1.3). SMRD = Southern Muskox Ridge diapir (Fig. 4). The belt developed in late Cretaceous and early Tertiary (Thorsteinsson and Tozer, 1970).

rocks in which the mafic constituents initially form crude mesh structures about altered felsic mega-crysts.

In contrast to anhydrite strata, igneous plutons in metamorphic complexes have various initial shapes and orientations which are difficult to reconstruct. Most importantly, strained anhydrite commonly exhibits relict bedding which marks the paleo-hor-izontal plane. This kind of reference plane, which is rarely present in granitoid rocks, provides important information about the total tectonic strain and as-sociated solid-body rotation (Ramberg 1959, van Berkel et al. 1986).

Shape fabric and strain analysis within anhydrite rocks

Undeformed anhydrite rocks underlying the prairies of North America and similar terrains elsewhere exhibit a type of internal structure variously de-scribed as nodular, mosaic or polygonal, and com-monly compared to chicken wire mesh. The dark mesh is composed of anhydrite and carbonate ma-terial, and often attributed to postdepositional de-hydration of primary gypsum (Riley and Byrne 1961, Murray 1964, Borchert and Muir 1964, p. 131). Anhydrite nodules can also form subaerially, in arid tidal flats or sabkhas (Dean et al. 1975, Kins-man 1966, p. 307).

The nodules generally account for >80 % of the rock volume and are therefore potential gauges of total tectonic strain (van Berkel et al. 1986, Robin and Torrance 1987). The pretectonic nodule fabric seems to be anistropic in most terrains, and its state of anistropy may be treated as a virtual flattening strain (I) in the plane of bedding. Robin's (1977) analytical method is therefore ideally suited for de-termining the nodule shape fabric in flat-lying as well as folded strata.

The calculation of total tectonic strain depends critically on accurate knowledge of the pretectonic nodule fabric. If the final shape fabric of strained nodules (foliation and lineation) is parallel or per-pendicular to the bedding plane then it can be rep-resented by a symmetric Cartesian tensor (T) and generated by coaxial or orthogonal superposition of the total tectonic strain (J) onto the virtual strain (van Berkel et al. 1986). Employing suffix notation and principal reference axes (1, 2, 3) we obtain

$$
\begin{aligned}
T_1 &= J_1 I_1 \\
T_2 &= J_2 I_2 \\
T_3 &= J_3 I_3
\end{aligned}
\tag{1}
$$

Given suitable fabric evidence, J can sometimes be split into two finite increments (K and L) of tectonic strain. Calculation of L depends only on T and KI, the tensor product representing the concordant nodule fabric at the onset of the final increment of straining. This means that L can be determined even if I is unknown. A practical example will be presented in which L has been crudely estimated by using T and KI. L will be a strain increment due to regional folding and KI the shape fabric after early diapirism.

Near-isotropic nodule fabrics

The nodular anhydrite of the >450 m thick, Carbo-niferous Otto Fiord Formation (Figs. 2a and 2b) apparently formed by the dehydration of primary gypsum during subsidence of the Sverdrup Basin (Nassichuk and Davies 1980, p. 69). The Otto Fiord anhydrite contains many limestone (Fig. 2a) which provide an independent check on magnitudes and directions of tectonic strain (Schwerdtner and Clark 1967). However, the interbeds are undisrupted and commonly show few signs of macroscopic defor-mation where the extreme axial ratio of nodules is <2.5.

The long axes of crudely aligned nodules are gen-erally parallel to bedding, but occasionally define a transverse fabric (Fig. 2c). This increases the uncer-
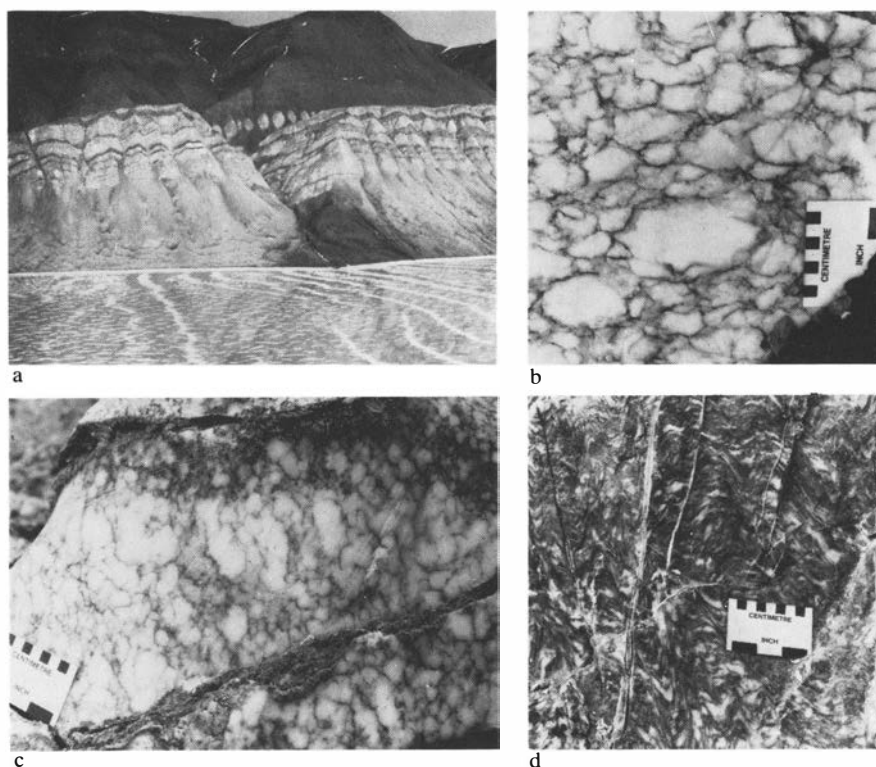
Figure 2: a. Bedded anhydrite in the middle segment of Van Hauen thrust, N.W. Ellesmere Island (Fig. 1). *b.* Nodular anhydrite, SW end of Blue Mountain thrust. *c.* Anhydrite nodules slightly elongated normal to bedding. Middle segment of Van Hauen thrust (Fig. 1). *d.* Mylonitic anhydrite, about 15 metres above middle segment of Van Hauen thrust.

tainty as to the state and variation of pretectonic nodule anisotropy, and greatly hampers the interpretation of final nodule fabrics in terms of total tectonic strain. It still remains to be demonstrated that all pretectonic nodule fabrics were concordant to bedding and had mean axial ratios of <1.5 (van Berkel et al. 1986). Evidently, a detailed study of nodule shapes needs to be made in flat-lying nodular anhydrite strata which have not been affected by diapirism, regional folding or severe faulting.

Natural lubricant

The Otto Fiord anhydrite lies along three reverse faults or listric thrusts in the Eureka Sound fold-and-thrust belt of early Tertiary age (Fig. 1). The crooked Stolz thrust (Nassichuk and Davies 1980, van Berkel et al. 1983) is poorly exposed, but juxtaposes Carboniferous and Tertiary strata at the present erosion level with an apparent stratigraphic throw of close to 10 km (Thorsteinsson 1974, Map
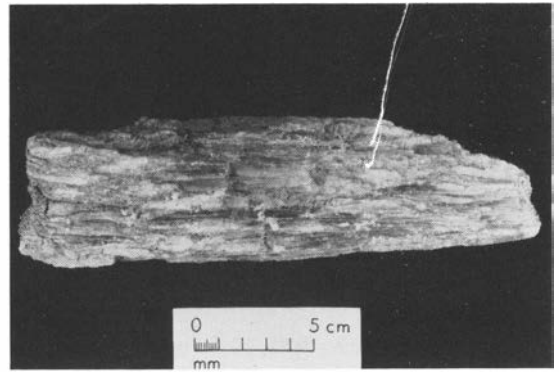
1302A). The Blue Mountain and Van Hauen thrusts (Fig. 1) are well exposed in several V-shaped valleys and juxtapose Carboniferous with lower Triassic strata. These two thrusts dip in opposite directions and are intimately related to adjacent large folds (Thorsteinsson 1974, Map 1309A, 1311A).

The anhydrite masses which overlie the Van Hauen and southern Stolz thrusts are inclined multi-order folds with hinge planes subparallel to the thrusts. The folds were produced in the Tertiary by (i) ductile shear of horizontal beds or (ii) detachment and tight oppression of the caps of low-amplitude salt walls formed in the Mesozoic (Jackson and Halls 1985, van Berkel et al. 1983, figs. 2 and 11). Accordingly, the clastic strata on the steepest flank of the salt walls were rotated, attenuated and finally disrupted in the Tertiary Eurekan Orogeny (Thorsteinsson 1974). This scenario may also apply to parts of the Blue Mountain thrust.

On all three thrusts, the anhydrite is crossed by many strike-slip faults which are rarely seen on aerial photographs but create a step-like map pattern of the Otto Fiord Formation (van Berkel et al.

Figure 3: a. Limestone fragments within gypsum, Blue Mountain thrust. Note hammer head at lower left corner. *b.* Selenite blades between limestone fragments, southern Stolz thrust (Fig. 1). *c.* Gypsum augen, same locality as Fig. 3b.

1983, fig. 9). The detailed macro-structure of the bedded anhydrite proves to be very complicated, and must be further analysed in well-exposed areas.

At this stage of research, three generalizations can be made regarding the lubricant role of anhydrite on the Blue Mountain and Van Hauen thrusts:

(1) The limestone beds have only locally been disrupted within the upper half of the anhydrite masses where deformation magnitudes are relatively low.

(2) Mylonitic anhydrite (Fig. 2d) and severely strained nodule fabrics are generally confined to the lower 50 m of Otto Fiord Formation present above the fault plane.

(3) The thrust plane is generally marked by foliated gypsum rock containing limestone fragments (Fig. 3a) and other evidence of severe deformation. The foliated gypsum is generally <8 m thick.

Aligned synkinematic selenite blades have grown between some limestone fragments (Fig. 3b). Elsewhere, the gypsum grain fabrics resemble those of augen gneisses (Fig. 3c) and preclude the possibility that gypsum is a surficial weathering product. Evi-

dently, the active zone of high contact strain became narrower as the Otto Fiord Formation of the hanging-wall block approached the earth's surface. The limestone beds of the Otto Fiord Formation are folded and boudiné throughout the entire anhydrite body that marks the southermost segment of the Stolz thrust. In contrast, the anhydrite bodies upon the Blue Mountain and Van Hauen thrusts are characterized by continuous planar limestone beds as well as anhydrite rocks which exhibit well-preserved primary and diagenetic structures (Nassichuk and Davies 1980). Boudins and small-scale folds in limestone beds are generally confined to the lower third of these anhydrite bodies. This seems to suggest that the magnitude of apparent stratigraphic throw is crudely proportional to the thickness of the zone of contact strain within the Otto Fiord anhydrite. Apparently, the ductile-strain level decreases rapidly, away from the fault plane and associated narrow mylonite zone, and probably remains below 30 % extension in the upper half of the anhydrite bodies resting on the Blue Mountain and Van Hauen thrusts. The bedded anhydrite is overlain conformably by competent clastic and carbonate rocks showing little sign of ductile deformation (Thorsteinsson 1974). At the top of the Otto Fiord

Figure 4. Lineated nodule fabric, Torvan syncline (see text and Fig. 5).

Formation, the inherent ductility contrast between evaporites and overlying rocks led to local stress concentrations and moderately-large strains in the uppermost anhydrite.

Natural analogue of strained metaplutonic rocks

Mylonitic anhydrite from large faults has experienced high strain that varies on the scale of <5 cm (Fig. 2d) and renders the attenuated and folded nodules unsuitable for shape fabric analysis (see also van Berkel et al. 1986, fig. 8). Nonetheless, such rocks illustrate that extreme non-coaxial deformation culminates in a finite increment which actively folds the planar shape fabric developed by the preceeding progressive strain. This phenomenon is common in uniform metaplutonic rocks and provides an important clue to the actual path of their ductile deformation.

As originally shown in laboratory experiments (Paterson and Weiss 1966), rocks with a strong strain-induced anisotropy are apt to buckle on the centimetre scale when subjected to tangential compression. Weakly-strained rocks, on the other hand, may remain mechanically isotropic and therefore capable of passive reshortening under tangential compression. Given appropriate magnitudes of reshortening, a planar shape fabric can be readily transformed into a linear shape fabric. This is plausible in weakly deformed anhydrite but seems questionable where the total strain is high (Fig. 4). How can one ascertain, in the absence of natural gauges of incremental strain, that a prolate nodule fabric was actually caused by passive reshortening of an oblate nodule fabric?

Two important conditions must be fulfilled to ac-

complish this task, (i) the kinematic path must be constrained by independent evidence, and (ii) the physical integrity of the nodules must have been retained throughout ductile deformation. These conditions are actually met within the folded anhydrite cap (Fig. 5) of a diapiric salt wall in the westernmost part of the Eureka Sound fold-and-thrust belt (Torrance 1986, Figs. 28−31).

Final nodule fabrics in the folded anhydrite cap of the southern Muskox Ridge diapir (SMRD)

The SMRD is located at the western boundary of the Eureka Sound fold-and-thrust belt and extends SE from Expedition Fiord into the Strand Fiord region on western Axel Heiberg Island (Figs. 1 and 5). The map pattern of the anhydrite cap and adjacent clastic strata leaves little doubt that the SMRD was highly affected by the regional buckle folding (Ramberg 1963, 1964) caused by E-W compression in the Eurekan Orogeny. The train of N-S buckle folds southwest of the diapir was effectively decoupled from the Expedition syncline by the evaporite wall (Fig. 5), thereby imposing a zone of sinistral ductile shear on the NE portion of the SMRD (van Berkel 1986, fig. 8.2).

The Strand Bay region contains several N-S salt walls with linear caps that could not be folded by regional E-W compression (van Berkel et al. 1984). These caps are dominated by subvertical oblate fabrics (Flinn 1965) which are concordant to bedding and thought to correspond with the prefold nodule fabrics in the SMRD (Schwerdtner et al., in review). Discernable weak lineations are generally subvertical.

Any nodule fabric can be quantified by a pair of independent scalars (r = intensity of shape anisotropy and k = prolateness factor) commonly used in finite-strain analysis (Flinn 1962, Watterson 1968). If a $\geq$ b $\geq$ c are the mean diameters of the final nodules in the principal directions of shape anisotropy, then for the final nodule fabric,

$$r(T) = (a/b) - (b/c) - 1$$
$$k(T) = [(a/b)-1]/[(b/c)-1] \qquad (2)$$

Both K (diapiric strain) and the prefold fabric probably varied throughout the SMRD, independently of the later buckling strain (L).

Quantitative shape analysis of the final nodule fabric shows that the maximum degree of measurable shape anisotropy, among the planar concordant fabrics in the unfolded diapirs, is nearly the same as
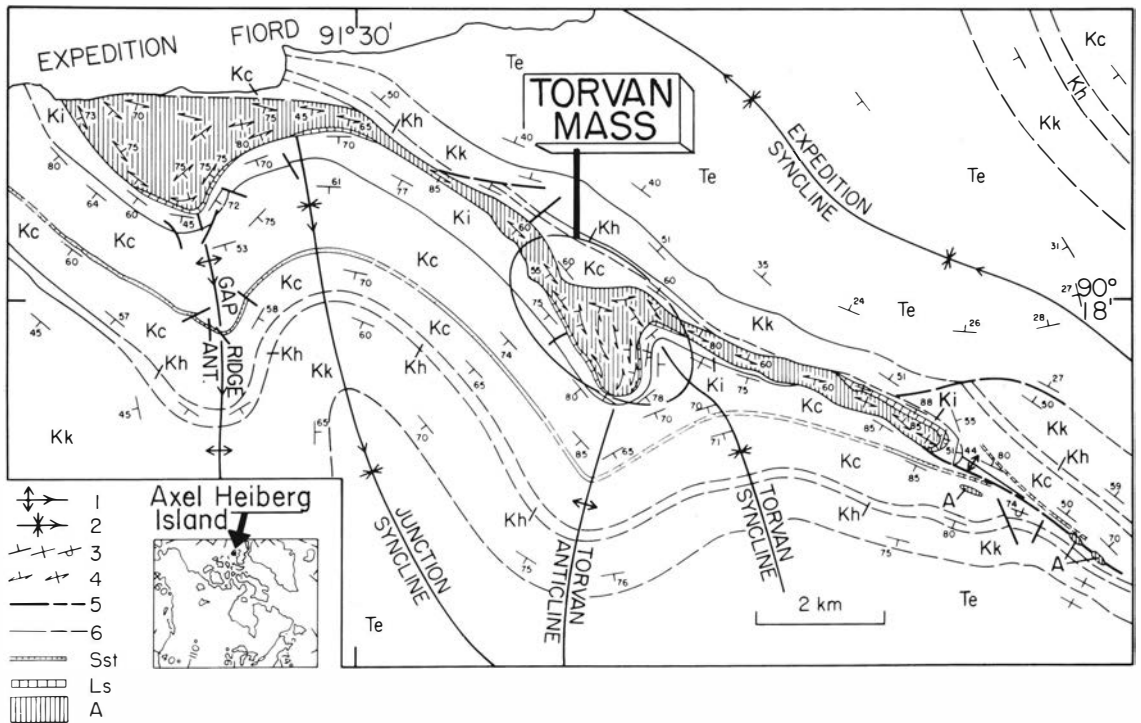
Figure 5. Southern Muskox Ridge diapir (Fig. 1, after van Berkel 1986, fig. 8.1). Maximum topographic relief is 500 m. Te: Tertiary Eureka Sound Formation (mostly sandstone and siltstone), Kk: Cretaceous Kanguk Formation (mostly siltstone and shale), Kh: Cretaceous Hassel Formation (sandstone), Kc: Cretaceous Christopher Formation (shale with minor sandstone beds, Sst), Ki = Cretaceous Isachsen Formation (mainly sandstone), A = Carboniferous Otto Fiord Formation (anhydrite with limestone interbeds), Ls = prominent limestone bed at top of anhydrite, 1: anticline, 2: syncline, 3: bedding (inclined, vertical, overturned), 4: Foliation defined by strained nodules (inclined, vertical), 5: fault (defined, inferred), 6: geological boundary (defined, inferred).

that in the folded NW-trending SMRD (Torrance 1986, figs. 27–30 and Appendix C). Field mapping revealed that the planar nodule fabrics in the Gap Ridge and Torvan anticlines bend around high-order (Ramberg 1964) flexural folds, together with relict limestone beds (Schwerdtner et al., in review). The flexural shear mechanism (Ramsay 1967, p. 391) accounts ·for the apparent lack of change in measurable r-value between the unfolded N-S diapirs and the SMRD (cf. Schwerdtner 1974, fig. 3). In other words, $r(KI) \sim r(T)$ in most of the SMRD, and L is represented by small-scale folds rather than being a contributor to the final shape of oblate-nodule fabrics.

The south-western contact zone of the Torvan anhydrite mass (Fig. 5) is dominated by prolate subvertical nodules with low r-values (van Berkel 1986, figs. 8.3–8.5). This zone contains the most prolate fabrics documented within the SMRD and is therefore unique within the Strand Bay region. The

correspondence between low r-values and high k-values is clearly apparent in a plot of all nodule fabrics measured within the Torvan anhydrite mass (Fig. 6).

Five ways were considered of producing the final fabrics of the southwestern contact zone of the SMRD from oblate prefold fabrics of nodule shapes (Fig. 7). The first three ways correspond to coaxial superpositions of L upon ideal oblate spheroids, which represent vertical oblate nodules prior to regional folding. Ways 4 and 5 (oblique pure shear and simple shear) are oblique superpositions in the horizontal plane and can lead to marked obliquities between bedding and principal directions of the final shape anisotropy (van Berkel et al. 1986). Such obliquities are very rare in the SMRD, which rules out ways 4 and 5 (Fig. 7).

The prolate concordant fabrics of the southwestern contact zone possess appropriate r/k values and orientations to have been produced by E-W passive
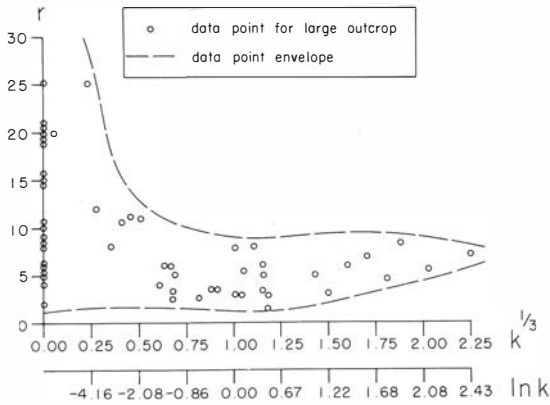
Figure 6. Plot of r versus k of nodule fabric, Torvan mass (Fig. 5). Based on field measurements by J.T. van Berkel and J.G. Torrance in 1984.
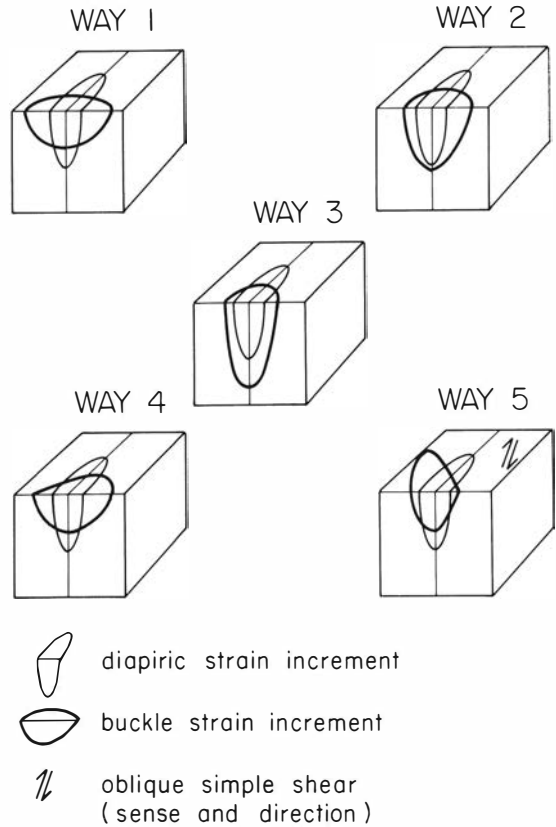

Figure 7. Five ways of producing vertical prolate ellipsoids (not shown) from vertical oblate spheroids representing the diapiric strain as well as the prefold nodules (no virtual strain). Way 1 = pure shear within the horizontal plane, way 2 = pure shear within the NW-SE vertical plane, way 3 = vertical constrictive, way 4 = obliquely superimposed pure shear in the horizontal plane, way 5 = horizontal simple shear in the vertical plane but oblique to the prefold spheroids.

shortening of subvertical oblate fabrics. If this shortening occurred during the N-S buckling of steeply-dipping strata then the natural r/k values should be explicable by a horizontal pure shear that is concordant to bedding and parallel to the SW contact of the SMRD (way 1 in Fig. 7). This proves to be the case for subvertical oblate spheroids (KI) with axial ratios and r-values between 6 and 27 (Fig. 8), the upper range in shape anisotropy degree obtained by laboratory analysis of planar nodule fabrics from unfolded N-S diapirs (van Berkel et al. 1986). Ways 2 and 3, (Fig. 7) include large components of vertical extension and cannot account for the low r-values of the prolate final fabrics (Fig. 8). The proximity of the competent Isachsen sandstone (Fig. 5) apparently assured a passive horizontal redeformation of the adjacent anhydrite in the early stages of regional N-S buckling and delayed the high-order folding of competent limestone interbeds (Schwerdtner et al., in review).

Apart from the r/k values, the kinematic path (Fig. 7) is also constrained by the empirical limit of nodule shape anisotropy, which is reached at extreme axial ratios of 25–30. Field measurements show that oblate anhydrite nodules with higher axial ratios have lost their identity and coalesce into discrete layers bounded by dark laminae. Clearly, such planar features cannot be reshortened into prolate nodules.

The largest r-value of prolate (k = 11.34) final fabrics measured in non crenulated nodular anhydrite is 7.17 (Figs. 4 and 6). The destraining of this final fabric with a/c = 10 and b/c = 1.5 by reciprocal pure shear in the horizontal plane (way 1) leads to r-values of the prefold fabric r(KI) which vary strongly with the precise k-value of the prefold fabric (r(KI)). Let $d \geqslant e \geqslant f$ be the mean principal diameters of the prefold nodules, and L (buckle fold strain) due to horizontal pure shear, i.e. a = d and bc = ef. Then eqs. (2) become

$$r(KI) = (a/e) + (e^2/bc) - 1 = (af/bc + (bc/f^2) - 1$$
$$k(KI) = [(a/e-1]/[e^2/bc)-1] =$$
$$[(af/bc)-1]/[(bc/f^3)-1] \qquad (3)$$

For example, if k(KI) = 0 then r(KI) = 66.67 but if k(KI) = 0.03 then r(KI) = 24.67. This corresponds to horizontal axial ratios b/c of 66.67 and 24.00, respectively, for the prefold oblate nodules. Note that the d/f values are 66.67 and 40.00, respectively, but are irrelevant to finding the limit of passive reshor-
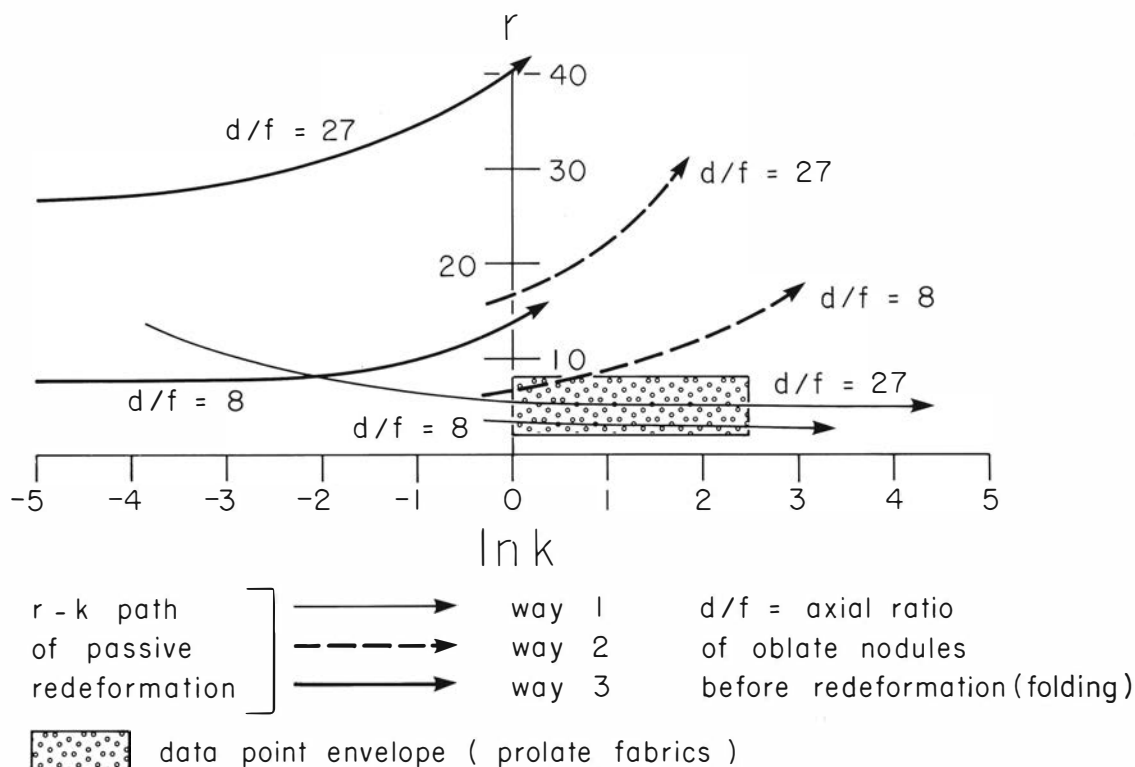
Figure 8. Passive redeformation of preflattened nodules (perfectly oblate disks parallel to bedding, not shown in the figure). Note that the r/k paths of way 1 (horizontal pure shear concordant to bedding) pass through the rectangle containing all data points obtained for prolate nodule fabrics in the Torvan mass (Figs. 5 and 6). Ways 2 and 3 correspond to pure shear in the NW-SE vertical plane and uni-axial vertical extension (constrictive deformation), respectively, which lead to exaggerated r-values. Oblique buckle strain results in final nodule fabrics that are discordant to bedding and therefore inap-propriate for the SMRD.

tening in the horizontal plane. Yet the natural example (Fig. 4) under discussion shows well-defined nodules in the a/c plane so that its prefold fabric was probably less oblate and anistropic than assumed above, e.g. $k(KI) = 0.16$, $r(KI) = 11.93$ $d/f = 26.32$ and $e/f = 10.40$.

Finally, L_1/L_3 can be calculated by deviding the two nodule ratios that apply to the horizontal plane and inverting the value thus obtained. Accordingly,

$$L_1/L_3 = [(a/c)/(e/f)]^{-1} \qquad (4)$$

Equation (4) yields a value of $L_1/L_3 = 6.90$, which is the pure shear increment associated with the re-gional buckle folding. This value is at best a first approximation to the actual strain increment, but its magnitude seems realistic. The values of L_1/L_2 and L_2/L_3 could be easily calculated because $L_2 = 1$ and there is no volume change in pure shear.

Conclusions

Nodular anhydrite is strained to various degrees in folded Mesozoic diapirs and Tertiary thrust sheets of the Eureka Sound belt in the Canadian High Arc-tic. The anhydrite is strongly mylonitic within a few metres of major thrusts, but the intensity of tectonic strain diminishes upwards (and away from the thrusts) to insignificance within 50−100 metres.

Many diapirs seem to have been folded or sheared in situ. One folded evaporite wall offered excellent exposures and was analysed in detail. This folded diapir is spatially associated with planar evaporite walls that are assumed to contain a record of the prefold nodule fabric. Based on this un-proven assumption, the final nodule fabric in the folded diapir is interpreted as being the net result of compaction, diapirism and regional folding.

Crude estimates can then be made of the folding strain in strongly reformed anhydrite.

Fabric analyses in the field and laboratory suggest that prestrained oblate nodules with mean axial ratios of up to 30 are still capable of passive reshortening without small-scale buckling, but whether this degree of passive behaviour extends to metatonalite and mea-diorite is not yet clear.

REFERENCES

Berkel, van, J.T. 1986: A structural study of evaporite diapirs, folds and faults, Axel Heiberg Island, Canadian Arctic Islands. *Published Ph. Thesis, University of Amsterdam, GUA Papers of Geology, Series 1, No. 26,* 149 pp.

Berkel, van, J.T., Hugon, H., Schwerdtner, W.M., Bouchez, J.-L. 1983: Study of anticlines, faults and diapirs in the central Eureka Sound fold belt, Canadian Arctic Islands: Preliminary results. *Can. Petrol. Geol. Bull., 31,* 109–116.

Berkel, van, J.T., Schwerdtner, W.M. and Torrance, J.G. 1984: Wall-and-basin structure: an intriguing tectonic prototype in the central Sverdrup basin, Canadian Arctic Archipelago, *Can. Petrol. Geol. Bull., 32,* 343–358.

Berkel, van, J.T., Torrance, J.G. and Schwerdtner, W.M. 1986: Deformed anhydrite nodules: a new type of finite strain gauge in sedimentary rocks. *Tectonophysics, 124,* 309–323.

Borchert, M. and Muir, R. 1964: *Salt deposits.* Van Nostrand Co., Ltd. London, 338 pp.

Dean, W.E., Davis, G.R. and Anderson, R.Y. 1975: Sedimentological significance of nodular and laminated anhydrite. *Geology, 3,* 367–372.

Flinn, D. 1962: On folding during three-dimensional progressive deformation. *Quarterly Journal of the Geological Society of London, 118,* 385–433.

Flinn, D. 1965: On the symmetry principle and the deformation ellipsoid. *Geological Magazine, 102,* 36–45.

Heim, A. 1958: Beobachtungen über Salzdiapirismus. *Ecologae Geologicae Helvetitiae, 51,* 1–32.

Jackson, K.C. and Halls, H.C., 1985: A test for the timing of folding of the North Mokka anticline using paleomagnetic data from diabase sills, eastern Axel Heiberg Island, Canadian Arctic Archipelago. *Bull. Can. Petrol. Geol., 33,* 227–235.

Kamb, B. 1970: Sliding motion of glaciers: Theory and observation. *Reviews of Geophysics and Space Physics, 8,* 673–728.

Kinsman, D.J.J. 1966: Gypsum and anhydrite of recent age, Trucial Coast, Persian Gulf. In: *Second Symposium on Salt, Northern Ohio Geol. Soc., 1,* 302–326.

Lotze, F. 1957: *Steinsalz und Kalisalze, Part 1.* Berlin, Gebr. Borntrager Verlag, 465 pp.

Müller, W.H. and Briegel, U. 1980: Mechanical aspects of Jura overthrust. *Ecologae Geologicae Helvetitiae, 73,* 239–250.

Müller, W.H., Schmid, S.M. and Briegel, U. 1981: Deformation experiments on anhydrite rocks of different grain size: rheology and microfabric. *Tectonophysics, 78,* 527–543.

Murray, R.C. 1964: Origin and diagenesis of gypsum and anhydrite. *Jour. Sedim. Petro., 34,* 512–523.

Nassichuk, W.W. and Davies, G.R. 1980: Stratigraphy and sedimentation of the Otto Fiord Formation. *Geol. Surv. Can. Bull., 286,* 87 pp.

O'Brien, C.A.E. 1957: Salt diapirism in South Persia. *Geologie en Mijnbouw, Nieuwe Serie, 19,* 357–376.

Paterson, M.S. and Weiss, L.E. 1966: Experimental deformation and folding in phyllite. *Bulletin of the Geological Society of America, 77,* 343–374.

Ramberg, H. 1959. Evolution of ptygmatic folding. *Norsk Geologisk Tidskrift, 39,* 99–151.

Ramberg, H. 1963: Strain distribution and geometry of folds. *Bull. Geol. Inst. Univ. Uppsala, 42(4),* 1–20.

Ramberg, H. 1964: Selective buckling of composite layers with constrasted rheological properties; a theory for simultaneous formation of several orders of folds. *Tectonophysics, 1,* 307–341.

Ramsay, J.G. 1967: *Folding and fracturing of rocks.* McGraw-Hill Book Company, New York, N.Y., 568 pp.

Riley, C.M. and Byrne, J.V. 1961: Genesis of primary structures in anhydrite. *Jour. Sedim. Petrol., 31,* 553–559.

Robin, P.-Y.F. 1977: Determination of geological strain using randomly oriented strain markers of any shape. *Tectonophysics, 42,* T7–T16.

Robin, P.-Y.F. and Torrance, J.G. 1987: Statistical analysis of the effect sample size on paleostrain calculation: I – Single-face measurements. *Tectonophysics, 138,* 311–318.

Schwerdtner, W.M. and Clark, A.A. 1967: Structural analysis of Mokka Fiord and South Fiord Jomes, Axel Heiberg Island, Canadian Arctic. *Canadian Journal of Earth Sciences, 4,* 1229–1245.

Schwerdtner, W.M. 1974: Erratum. Schistosity and mineral lineation as indicators of paleostrain directions. *Can. Jour. Earth Sci., 11,* 210.

Schwerdtner, W.M. and Osadetz, K. 1983: Evaporite diapirism in the Sverdrup Basin: New insights and unsolved problems. *Bull. Can. Petrol. Geol., 31,* 27–36.

Schwerdtner, W.M., van Berkel, J.T. and Torrance, J.G., (in review): Pattern of apparent total strain in the bedded anhydrite cap of a folded salt wall. *Journal of Structural Geology.*

Talbot, C.J. 1979: Fold trains in a glacier of salt in southern Iran. *Journal of Structural Geology, 8,* 5–18.

Thorsteinsson, R. 1974: Carboniferous and Permian stratigraphy on Axel Heiberg Island and western Ellesmere Island, Canadian Arctic Archipelago. *Geol. Surv. Can. Bull., 224,* 115 pp.

Thorsteinsson, R. and Tozer, E.T. 1970: Geology of the Arctic Archipelago. *In:* Geology and Economic Minerals of Canada, R. J.W. Douglas, ed., *Geol. Surv. Canada Economic Rt. 1,* 548–590.

Torrance, J.G. 1986: Structural geology of evaporite piercement walls and adjacent synclines, Axel Heiberg Island, Canadian Arctic Archipelago. *Unpublished M.Sc. thesis, University of Toronto, Toronto, Ontario, Canada.*

Watterson, J. 1968: Homogeneous deformation of the gneisses of Versterland, southwest Greenland. *Grönlands Geologiske Unders. Bull, 78,* 75 p.